

MISS CAMILA FERNANDEZ ZAPATA (Orcid ID : 0000-0003-4795-6053)

DR JOSEF PRILLER (Orcid ID : 0000-0001-7596-0979)

DR CHOTIMA BÖTTCHER (Orcid ID : 0000-0002-6226-586X)

Article type : Mini-Symposium

The use and limitations of single-cell mass cytometry for studying human microglia function

Camila Fernández-Zapata¹; Julia K.H. Leman¹; Josef Priller^{1,2,3}; Chotima Böttcher¹

¹Department of Neuropsychiatry and Laboratory of Molecular Psychiatry, Charité – Universitätsmedizin Berlin, Berlin, Germany

² German Center for Neurodegenerative Diseases (DZNE), Berlin, Germany.

³ University of Edinburgh and UK Dementia Research Institute (DRI), Edinburgh, UK.

Corresponding author:

Chotima Böttcher, Department of Neuropsychiatry and Laboratory of Molecular Psychiatry, Charité – Universitätsmedizin Berlin, Berlin, Germany (E-mail: chotima.boettcher@charite.de)

Keyword

Mass cytometry, imaging mass cytometry, human microglia, multiple sclerosis, depression, microglia function

ABSTRACT

Microglia, the resident innate immune cells of the central nervous system (CNS), play an important role in brain development and homeostasis, as well as in neuroinflammatory,

This article has been accepted for publication and undergone full peer review but has not been through the copyediting, typesetting, pagination and proofreading process, which may lead to differences between this version and the [Version of Record](#). Please cite this article as doi: [10.1111/BPA.12909](https://doi.org/10.1111/BPA.12909)

This article is protected by copyright. All rights reserved

neurodegenerative and psychiatric diseases. Studies in animal models have been used to determine the origin and development of microglia, and how these cells alter their transcriptional and phenotypic signatures during CNS pathology. However, little is known about their human counterparts. Recent studies in human brain samples have harnessed the power of multiplexed single-cell technologies such as single-cell RNA sequencing (scRNA-seq) and mass cytometry (cytometry by time-of-flight [CyTOF]) to provide a comprehensive molecular view of human microglia in healthy and diseased brains. CyTOF is a powerful tool to study high-dimensional protein expression of human microglia (huMG) at the single-cell level. This technology widens the possibilities of high throughput quantification (of over 60 targeted molecules) at a single-cell resolution. CyTOF can be combined with scRNA-seq for comprehensive analysis, as it allows single-cell analysis of post-translational modifications of proteins, which provides insights into cell signalling dynamics in targeted cells. In addition, imaging mass cytometry (IMC) has recently become commercially available, and will be useful for analysing multiple cell types in human brain sections. IMC leverages mass spectrometry to acquire spatial data of cell-cell interactions on tissue sections, using (theoretically) over 40 markers at the same time. In this review, we summarise recent studies of huMG using CyTOF and IMC analyses. The uses and limitations as well as future directions of these technologies are discussed.

INTRODUCTION

The cellular network of the human brain is highly dynamic and complex, yet well organised and controlled. Its cellular dynamics traverse between segregated and integrated states overtime, across different cell types and regions. Myeloid cells of the CNS include microglia and CNS-associated macrophages (CAM), as well as infiltrating monocytes, all of which are key players in this network. The origin and development of parenchymal microglia and CAMs (these are meningeal, perivascular and choroid plexus macrophages) are well studied in the mouse CNS (28, 29, 38, 48, 55, 72), whereas little is known about their human counterparts. Recently, a study using single-cell transcriptomic profiling has demonstrated that during early foetal development (gestational week [GW] 9 to 18) human foetal microglia are highly heterogenous (41). By mid-gestation (around GW13), foetal microglia display phenotypic profiles and functional properties of mature microglia, especially the gene programs necessary for immune-sensing, synaptic pruning, phagocytic and tissue-supportive functions. These findings suggest the importance of microglia during early foetal development, possibly in response to environmental perturbations during pregnancy. However, the origin of this cell population and a complete knowledge of its development remain to be investigated in the human system.

Studies in mouse models have also revealed microglia as important contributors to neuronal circuit formation and function during development, homeostasis and disease (64). They maintain brain homeostasis by shaping and protecting the structural and functional integrity of the CNS (48, 61, 74). Under disease conditions, microglia rapidly react to changes in their local environment and either become harmful to neurons or provide protection, resolving neuroinflammation and/or limiting neurodegeneration (64). Due to their wide range of phenotypes and functions, it has long been proposed that microglia display phenotypic and functional heterogeneity (26, 49). However, it remains elusive whether the diversity of specialised microglial subsets is a pre-existing feature of healthy human brains, or the result of context-dependent phenotypic and functional changes over time. Additionally, it is also not well understood how these unique microglial subsets respond under disease conditions. Understanding the mechanisms and factors that regulate microglial homeostasis and function may provide avenues for therapeutic intervention.

Recent advances in single-cell technologies such as single-cell RNA sequencing (scRNA-seq) have enabled characterisation of the complexity of human microglial transcriptional landscape (41, 48, 69). In the healthy adult brain, scRNA-seq revealed that adult microglia are commonly less heterogeneous, compared with microglia in developing brains (41, 48). Mature microglia exist in a spectrum, with no obvious distinction between transcriptional states, rather than unique subsets with distinct transcriptional profiles (48, 69). Homeostatic microglia could be identified by their expression of microglial core genes such as *TMEM119*, *CX3CR1*, *P2RY12*, and *SLC2A5* (48, 69). A rare microglial population was characterised by high expression of chemokine genes, including *CCL2*, *CCL4* and *IL1B* (48, 69). Furthermore, the distribution of the defined microglial subsets was shown to be region-dependent (69). Under CNS pathology, greater complexity of microglial subsets was observed. ScRNA-seq assessment of human microglia isolated from the brain biopsies of patients with multiple sclerosis (MS) defined microglial subsets which were associated with or enriched in the MS brain (48). MS-associated microglia downregulated microglial core genes *TMEM119*, *CX3CR1*, *P2RY12*, and *SLC2A5*, and had increased levels of expression of MHC class II-related molecules, such as *CD74*, *HLA-DRA*, *HLA-DRB1* and *HLA-DPB1*, *APOE*, *SPP1* and *MAFB* (48). Similarly, downregulation of the core genes including *CX3CR1* and *SELPLG* was also found in microglia from glioblastomas, determined by scRNA-seq (69). Glioma-associated microglia were characterised by different expression levels of hypoxia-associated genes such as *HIF1A* and *VEGFA*, the interferon-related gene *IFI44*, *SPP1*, *HLA-DRA*, *APOE*, or *CD163* (69), which again demonstrated microglial heterogeneity in the diseased human brain.

Together, single-cell transcriptional analysis showed heterogeneity of human microglia during early development and in the adult brain. These cells show context-dependent signatures in the diseased brain at the single-cell mRNA expression level. In addition to scRNA-seq assessment, single-cell proteomics/protein expression of human microglia has been successfully assessed using mass cytometry. In this review, we summarise recent findings on microglial heterogeneity and disease-associated diversity at the single-cell protein expression level, determined by CyTOF and IMC. We also discuss herein the uses and limitations of these techniques for future studies of human microglial function.

Use of CyTOF in single-cell huMG characterisation

CyTOF enables high-dimensional protein analysis of immune cells by way of antibodies bound to rare heavy metal isotopes, which label proteins of interest on the surface, in the cytoplasm and in the nucleus of cells (7). In Figure 1, we provide a diagram showing how CyTOF works. Briefly, the (metal-tagged) antibody-labelled cells are passed through a nebuliser to create single-cell droplets, which then are ionised using inductively coupled plasma (ICP). The ionised particles are passed through a quadrupole to remove cellular debris from the rare heavy metal ions, and are then quantified using TOF mass spectrometry (7). The output data shows which ions, and therefore specific antibodies, were associated with one cell. CyTOF can be used to study post-translational modification of proteins including protein phosphorylation in cell signalling (17, 53), which greatly complements a limitation of scRNA-seq. Cell signalling proteins and histones undergo phosphorylation, methylation, and acetylation as the cell responds to signals and activates different signalling pathways. Disruptions in histone acetylation were observed in the microglia of mice showing signs of depression following *Bacillus Calmette-Guérin* (BCG) vaccination (67). Single-cell immune phenotyping using CyTOF has been successfully combined with the analyses of histone modification patterns and epigenetic codes at the single cell level (17). This strategy is promising in that it provides highly comprehensive data, which would allow us to better understand the complex biology of the targeted cells.

While CyTOF has a clear advantage in terms of panel breadth when compared to flow cytometry, scRNA-seq data is much more highly dimensional. ScRNA-seq directly reveals all the transcripts expressed by a cell at that moment, without any biases that may result from panel design, marker (antibody) selection and affinity/specificity of the antibodies used. CyTOF experiments are still practically limited to around 60 markers (theoretically 120 markers) (32, 33, 50), meaning that researchers must still focus in on particular types or functions of cells. Another considerable limitation of this technology is significant variation in signal intensity over time and across

machines, which limits the application of CyTOF in multi-site or longitudinal studies. Nevertheless, normalisation methods and algorithms and the use of anchor samples have been developed to improve the reproducibility and comparability of CyTOF results across experiments and study sites (21, 39, 44, 77).

Use of imaging mass cytometry (IMC) in huMG characterisation

Recently, imaging mass cytometry (IMC) was developed by combining typical immunohistochemistry (IHC) techniques and mass cytometry to investigate samples in solid state (27). In IMC analysis, several tissue types such as fresh frozen and formalin-fixed paraffin-embedded (FFPE) specimens can be used. Samples mounted as a slice are stained with metal-tagged antibodies using IHC protocols with or without the use of antigen retrieval. Subsequently, regions of interest are selected from each sample and ablated with a UV laser at a resolution of 1 μ m. The resulting ionized mass is then fed to a time-of-flight (TOF) mass spectrometer and the metal abundances for each spot are recorded (Figure 1). The information for each spot is then tracked back to the original coordinates reconstructing an "image" from the original section, similar to what is obtained in fluorescence microscopy (27), with the advantage that (theoretically) around 40 markers can be measured simultaneously. Unlike CyTOF, in IMC the information acquired by the mass-spectrometer does not correlate with a single-cell but with a coordinate, thus a pre-processing single-cell segmentation step is needed for each image, in order to analyse the single-cell data. The information obtained from each sample allows for morphological, spatial and network analysis of cell subpopulations in relation to their local environment, enabling a detailed description of tissue architecture in healthy and pathological conditions at an unprecedented level of dimensionality. From a technical standpoint, there are several differences between CyTOF and IMC, which may impede a direct comparison of results obtained from the two technologies. The first is the throughput of data acquisition. CyTOF uses multiplexed samples commonly isolated from a large brain tissue (~ 2–10 g), allowing higher throughput than IMC, which images a single 1-mm² area of interest each time. Secondly, single cells analysed by CyTOF are isolated from brain tissue, thus resulting cell populations are influenced by the isolation protocol used. IMC analyses cell populations without a cell isolation step, and all cell types residing in the tissue can be analysed or detected with specific antibodies. Finally, there is usually no restriction of combining metal-tagged antibodies in CyTOF analysis, whereas tissue types (frozen or FFPE) and/or an antigen-retrieval protocol are the main factors affecting the antibodies compatible in one IMC panel. This restriction, in turn, limits the dimensionality of the IMC data (13). The advantages and limitations of IMC versus other imaging techniques have

been discussed elsewhere (27). Briefly, while some of the most widely used techniques can give a better resolution (e.g. electron microscopy, fluorescence-based IHC with confocal microscopic analysis), none of them can acquire such high number of markers simultaneously. The few other high-dimensional techniques have the disadvantage of either low resolution (MALDI) or much higher times of sample processing and acquisition, as in sequential immunofluorescence staining (SIFS). Although SIFS gives higher resolution and is theoretically able to acquire up to 60 markers from the same sample, it has disadvantages of large acquisition times (up to weeks in some cases), large datasets (which require high computational capacity), and a disturbance of certain antigens and/or area of interest between staining cycles which further hamper a quantification (78).

IMC has been used to study human cancer (3, 15, 25, 27), diabetes (19, 79), immune cell development (45, 84) and human microglia in multiple sclerosis (13, 60, 66). Although results obtained from recent studies on human microglia using IMC are still limited due to small sample cohorts and the number of investigated markers (13, 60, 66), these works demonstrate the power of this technology to study phenotypic changes of microglia and their correlation with spatial location in diseased brain at high-resolution. Nevertheless, continuing efforts to optimise and standardise IMC staining are needed. In particular, optimisation of antigen retrieval for IMC analysis of brain tissue is necessary to increase the number of investigated markers in one measurement, and thus enhances dimensionality of the data per measurement.

Experimental design and data analysis

Collection of human brain tissues

Commonly, human brain specimens can be obtained as autopsy tissues (12, 13, 23) or fresh biopsies, which are surgically resected, e.g. from patients with refractory epilepsy or brain tumours (12, 22, 30, 69). Collection of huMG for immune profiling study is complex and involves several contextual dependencies, including the specific disease context, biological hypotheses, types of brain specimen (fresh biopsy versus autopsy), the study and control groups, and sample preservation. Some of these aspects of experimental design are discussed in this section. In addition, in Figure 2 we provide a flow diagram of practical considerations often encountered when planning huMG collection and analysis, including sample processing and antibody staining. A significant challenge in investigations of huMG in both healthy and diseased brains is the selection of appropriate control tissue. Often, biopsy tissue is used as a control. Recently, we have demonstrated similarities and differences in microglial profiles between fresh biopsy (taken from the margins of epileptogenic focus) and autopsy tissues (12), determined by CyTOF. These

phenotypic differences could be explained by differences between live/biopsy versus post-mortem/autopsy tissue, or by differences between epileptic versus nonepileptic tissue. It has been shown that some properties of huMG from the epileptogenic focus and margins are comparable (83). Therefore, special care should be taken when the margins of the epileptogenic focus or brain tumours are used as “control” brain tissues. Other factors may also affect the phenotype of control and study MG. It has been shown in a study of brain autopsies from over 100 brain donors that the pH of cerebrospinal fluid (CSF) rather than age or post-mortem delay significantly affected microglial viability and possibly their phenotype (54). However, these conclusions were drawn based on few phenotypic markers, and thus may underestimate the changes induced by age and/or post-mortem delay, or may overestimate the effects of CSF pH. More markers need to be analysed to conclude anything definitive about the responses of microglia to changes in CSF pH. Nevertheless, it is advisable to report CSF-pH of the donors at the time of brain autopsy.

Several other aspects of sample collection, processing and storage should also be considered during experimental design. *In vivo*, spatiotemporal characterisation of longitudinal huMG studies, of the sort which are feasibly and repeatedly performed on inbred animal strains (29, 37, 38, 48), remain out of question for human studies. This means that an *ex vivo* study of huMG provides only a snapshot (in time and space) of their phenotypic and functional complexity. High inter-individual variability is also common in human sample cohorts, which can influence the interpretation of the resulting data. An experiment design involving several cell types and/or compartments (e.g. peripheral blood, cerebrospinal fluid and brain regions) from the same individual may increase the power of statistical analysis (e.g. by performing paired testing), as well as allow validation of antibody specificity intra-individually (for example PBMCs can be used as a negative control for P2Y₁₂-antibody staining (12)). Finally, although massive cell loss can occur during CyTOF measurement, we have demonstrated that it is feasible to analyse samples with a low cell number ($10^3 - 10^4$ cells) by using barcoding (multiplexing) prior to storage (12).

One of the major factors limiting research on human microglia is their susceptibility to cryopreservation damage and environmental changes. For example, cryogenic storage using freezing medium containing 10% dimethyl sulfoxide (DMSO) significantly affected cell recovery, phenotypes and RNA quality (54). Therefore, the phenotypic characterisation of huMG has long relied on low dimensional, immunohistochemical analysis of post-mortem brain tissue (commonly formalin-fixed paraffin-embedded [FFPE]) or fluorescence-flow cytometric analysis of freshly isolated or *ex vivo* cultures of huMG (51, 52, 54, 56, 62). Limitations of these approaches include the phenotypic changes induced by *in vitro* culture condition (30), the high autofluorescent background of post-mortem tissue and the restrictions in the number of markers that can be

simultaneously investigated at the same time (commonly less than 20). Alternatively, to minimise freeze-thaw-dependent changes in their phenotypic and/or functional states the isolated huMG may be fixed prior to cryopreservation (34). However, this strategy can reduce accessibility of some epitopes for antibody staining, thus validation is required before starting the sample collection. We have recently validated a protocol for long-term cryopreservation of isolated huMG and circulating immune cells from peripheral blood and CSF using Proteomic Stabilizer PROT1 (Smart Tube Inc.) (11, 12, 13), which has previously been used in a study of mouse microglia (2). Using our established protocols for cryopreservation and barcoding, immune cells from different compartments could be barcoded (multiplexed), pooled and fixed prior to cryopreservation, which allows simultaneous storage and analysis of different cell types from different compartments. Of note, some antibody clones may stain cells under these conditions better than the others, for example we could better detect the CD14 epitope of the PROT1-fixed cells with the clone RMO52 than the clone M5E2 (own unpublished data).

Single-cell isolation

One of the major challenges in studying huMG (or the other CNS-resident cells such as astrocytes or CAMs) is the isolation of targeted tissue-resident cells from brain tissues. It is crucial to obtain sufficient cell numbers and to prevent significant phenotypic and/or transcriptional deviation from the *in vivo* microglial signature, and this can be more challenging when isolating tissue-resident cells, as opposed to those in the circulation. It has been reported for both mouse and human microglia that shortly after isolation (hours) or culture, microglia downregulated their unique signature and also altered their functional phenotype (9, 30). Treating microglial cultures with the transforming growth factor β 1 (TGF- β 1) has been shown to provide modest effects in promoting an *in vivo* pattern of microglial transcriptional landscape (30). However, molecule(s) that could restore full *in vivo* homeostatic and functional properties of huMG remain to be identified, and it should be kept in mind that these may interfere with additional phenotypic characteristics of huMG.

In general, huMG single-cell suspensions can be obtained from brain tissues using an isolation protocol involving either enzymatic digestion (usually a collagenase/DNaseI solution) (11, 12, 13, 22, 51, 54, 58) or mechanical dissociation (23, 30, 58, 69). Although it has been demonstrated that enzymatic dissociation (especially trypsinisation) greatly affected some CNS-resident cells such as protoplasmic astrocytes (16), this strategy had little effect on microglia and did not influence the specificity of the antibody staining (12, 58). In our experience, to achieve sufficient cell numbers and retain cellular heterogeneity for CyTOF analysis, an enzymatic digestion is required for the isolation of huMG from some brain regions such as the subventricular zone, and

for the isolation of CAMs such as perivascular macrophages and choroid plexus macrophages (12). After obtaining a single-cell suspension, isolated cells are separated from myelin and cell debris using Percoll density gradient centrifugation. However, since TOF mass spectrometry is more sensitive to cell debris/clumps (compared to flow cytometry), and a fraction of Percoll-pre-isolated cells is often still contaminated by the presence of remaining myelin and cell debris, a step of cell enrichment such as the magnetic-activated cell sorting (MACS®) or fluorescence-activated cell sorting (FACS™ or flow cytometry) can be included following Percoll pre-isolation (11, 12, 13). When analysing cells using CyTOF, it is also critical to control cell viability and integrity before and during CyTOF measurement, which also means before and after cryopreservation. In CyTOF analyses, cell viability can be assessed through covalent binding of the platinum-containing chemotherapy drug cisplatin (20) or the palladium-based covalent reagent dichloro-(ethylenediamine) palladium (35). These compounds preferentially label nonviable, membrane-compromised (dead) cells. Together with the use of metal-containing intercalators (59), which label cellular DNA content, live and dead cells can be distinguished. In addition, apoptotic markers such as cleaved caspase-3 and cleaved poly(ADP-ribose) polymerase (cPARP) can be used to confirm cellular integrity.

Antibody panel

Compared to scRNA-seq data, CyTOF data is much less high-dimensional and affected by the markers included in one measurement. Antibody panel design is crucial for cell subset identification and/or exclusion and for direct comparisons between studies. Recently, we have demonstrated the similarities and differences in clusters/subsets identified in the same sample using different antibody panels (10, 11, 12, 13, 85). An overlap of a set of phenotypic-defining markers (often designated as *TYPE* markers) between experiments can be used to facilitate the comparison of cell clusters/subsets between experiments (13). Although over 400 metal-conjugated antibodies for CyTOF and more than 100 antibodies for IMC are commercially available from Fluidigm (www.fluidigm.com), antibodies recognizing most of the huMG-related markers including P2Y₁₂, TMEM119, Clec7a, TREM2, EMR1 and GPR56 are not available as metal-tagged format. However, metal conjugation of antibodies can be easily performed using for example a commercially available Maxpar® antibody labelling kit (www.fluidigm.com) or previously published protocols (36). Selected antibodies should be then assigned to available channels according to the expected abundance of the targeted protein and the signal delivered to the detector. For the optimal delivery of metals to the detector, the ion optics within the CyTOF instrument is tuned in the 153-176 Da range. While signal spillover in CyTOF is much less compared with fluorescence-based flow cytometry, natural isotopic impurity (*m*+1, *m*+2, etc.)

and/or the oxidation of elements during measurement ($m+16$) should however be considered in panel design. More details on panel design for a CyTOF study are described elsewhere (43, 75, see also Maxpar Panel Designer, www.fluidigm.com).

HuMG subset identification and analysis

Prior to data analysis, CyTOF data must undergo some pre-processing steps (Figure 3). Many CyTOF experiments take advantage of the Palladium-based mass tag barcodes for sample multiplexing (86). The de-barcoding step can be done using available platforms such as FlowJo (www.flowjo.com) or Cytobank (www.cytobank.org). Although the use of metal-labelled antibodies drastically reduced channel crosstalk as compared with the use of fluorophores in flow cytometry, signal spillovers can still occur between channels, thus signal compensation is required to enable the correct interpretation of the data. Signal spillovers can be compensated using the CATALYST package (18) in R (65). Prior to data visualisation, we normally apply the arcsinh (hyperbolic inverse sine) with cofactor 5 transformation to account for deceptive effects of low protein expression signals and facilitate distinction between positive and negative populations (10, 11, 12, 13). The pre-processed data can be then visualised into an interpretable reduced-dimensional space using for example the t-stochastic neighbour embedding (tSNE) algorithm (4, 47) and the uniform manifold approximation and projection (UMAP) (6) or a multilevel layout algorithm such as the force-directed layout (FDL) available in VortexX (<https://github.com/nolanlab/vortex>) (68). To further identify different cell states/subsets as well as to take analysis-related variability of CyTOF data between studied groups into account, several algorithms for clustering analysis have been developed.

Unsupervised clustering is well suited for exploratory studies of tissues in which the immune populations of interest have been poorly defined. These clustering methods have been developed to cluster cells into subsets based on the expression of the proteins studied, with minimal guidance from the researcher. Unsupervised clustering has been shown to reliably separate well-studied populations of cells from each other, but the real value of this technique lies in its ability to identify novel, often rare populations that are missed due to the biases and conventions of biaxial gating (10, 11, 12, 13). Nonetheless, unlike the clustering analysis of data obtained from scRNA-seq, clustering CyTOF data is dependent on the pre-selection of proteins analysed in one panel (which is usually limited to around 40), thus identification of cell populations largely relies on panel design. Also, in our opinion, the identified huMG clusters remain descriptive and could possibly be interpreted as distinct microglial subsets or transient cell states. Further functional analysis and/or cellular spatial resolution of each identified cluster are essential. In this current

review, we describe two exploratory meta-clustering analyses that we commonly used in our laboratory: *FlowSOM/Consensus-ClusterPlus* (57, 76, 81) and *VorteX* (68).

FlowSOM (76) and *ConsensusClusterPlus* (81) are among the fastest and best-rated clustering algorithms and are part of common CyTOF workflows (57) adapted to the R environment (65). *FlowSOM* applies the principles of self-organizing maps (SOM), in which maps are specific types of artificial neural networks, consisting of a grid of nodes (or points in the multidimensional space), assigning each data point to the node that is its nearest neighbour. In the workflow established by Nowicka *et al.* (57), *FlowSOM* combines all cells from all samples and organizes them in an initial grid of 100 nodes. These first 100 nodes are then used by *ConsensusClusterPlus* to create subsequent meta-clusters, which facilitates readability and biological interpretation of the clusters. The selection of the correct number of clusters is not automatic and it is recommended to either cluster the data according to an expected number of cell types (useful, for instance, when analysing peripheral blood cells) or to apply the "elbow" criterion (explained in the *VorteX* description below). Overclustering approaches, in which the number of clusters selected is higher than expected, may on one hand be useful for exploratory studies (detecting of a rare cell population). On the other hand this approach may result in fragmenting the biologically bona fide subsets and reducing cluster reproducibility between runs. In our CyTOF studies (10, 11, 13), we applied this strategy to explore rare cell populations and/or cell states in disease conditions, which may have remained uncovered otherwise.

VorteX is an open-access platform which uses an unsupervised clustering algorithm, X-shift, to cluster data points according to the variables (markers) that were analysed (68). X-shift uses k-nearest neighbours density estimation (kNN-DE) to assign cluster centroids to areas with a high density of data points, and then the remaining data points are connected to their nearest centroids. k represents the number of nearest neighbours which are considered during clustering, meaning that the k-value is inversely related to the number of clusters. A low k-value will result in better resolution of small or similar clusters, but these clusters will be more susceptible to stochastic variation. Validating the number of clusters which best reflects the structure of a dataset is an important part of any clustering analysis. The number of clusters is determined by finding the point (known as the elbow point) where increasing the number of clusters does not explain any more of the variation in the data. This point can be calculated by plotting cluster number over k, and using line-plus-exponent regression (68). *VorteX* has several in-built visualisation tools for analysis. The force-directed layout (FDL) is used to plot every data point in the dataset (or 1000 randomly sampled events from a cluster with >1000 points), and information about marker expression, cluster ID or sample origin can be overlaid. Cells will exert an attractive force on other cells of a similar phenotype, and a repulsive force on those with a different

phenotype, meaning that similar clusters will be grouped together. This method of visualisation differs from other visualisation tools which use dimensionality-reduction, because the full dimensionality of the data is considered during plotting. The attractive and repulsive forces mean that the data points are much less evenly distributed than in a tSNE plot. Another analysis tool available on VorteX is the divisive marker tree (DMT). This is a hierarchical classification tree which uses binary division to split clusters from the central node containing all the clusters. The DMT shows the markers which distinguish one cluster from another, to give an indication of cluster phenotype (68). The main limitation of VorteX is the amount of computing power required to cluster datasets of over one million cells. For large cohorts of data, or samples with many cells either down-sampling or a computer with a large amount of random-access memory (RAM) is necessary.

In the case of IMC data analysis a segmentation step is necessary to access single-cell information. IMC raw data (.mcd files) can be easily extracted as .tiff files or .csv files for further processing. In our current workflow image segmentation (13) is performed on .tiff files using the pixel classifier *llastik* (8) in which the algorithm is trained by the user to distinguish different cell compartments such as cytoplasm, membrane and nuclei from background based on marker expression. *llastik* produces single-cell binary masks for each image that can be then fed to *CellProfiler*, (14) where one can either obtain the single cell data from each sample in the form of .csv files or transfer single-cell masks readable by *histoCAT* (70). *HistoCAT* is an open-source interactive computational tool specifically designed for IMC analysis that incorporates high-dimensional image visualisation and different analysis methods for cell phenotype characterisation (such as tSNE plots or PhenoGraph clustering) as well as tools for study of cell-cell interactions and cell complex networks. Finally, single-cell data can be extracted from *histoCAT* in .fcs files that can be analysed using common CyTOF workflows (as mentioned above, Figure 3).

One of the current limitations of CyTOF technology is the considerable variation between experiments, which hampers longitudinal studies or studies of a large patient cohort. This is in part due to changes of signal intensity during measurement, which can be resolved by using normalisation beads in each measurement. In addition, variations in results/signals may also be caused by sample preparation and/or *in vitro* stimulation prior to CyTOF acquisition, and the variation in antibody master mixes between experiments. Several steps of standardisation and normalisation are therefore required to achieve a reliable dataset. These steps include for example 1) the cryopreservation of samples (which is technically challenging for tissue-resident cells such as microglia) (12); 2) the use of anchor samples, which allows direct estimation of batch effects between runs (73) but may not be feasible for some types of human cells due to

their accessibility; and 3) premixing of antibody cocktails followed by cryopreservation and storage, which has been proven to improve signal consistency between runs (71). Finally, lots of efforts have been made to develop new pipelines for identification and normalisation of batch effects. One of such approaches is *CytoNorm* (77), which includes the use of anchor samples, accounting for the different biological settings used in the study, and an algorithm that corrects for batch-to-batch variability. Some studies have already proven the potential reproducibility of the technique, showing multi-site PBMC and whole-blood comparability (5, 44). However, this workflow or the other normalisation protocols has never been applied to huMG studies.

Recent findings on huMG heterogeneity in health and diseases, determined by CyTOF and IMC

Regional heterogeneity

Albeit much less frequently in the literature than scRNA-seq technology, several CyTOF and IMC studies on huMG and/or human brain specimens have recently demonstrated the power of these single-cell high-dimensional technologies to explore huMG phenotypes and functions in health and diseases (11, 12, 13, 60, 66, 69), as summarised in Figure 4.

In-depth immune profiling by CyTOF revealed distinct phenotypes of huMG isolated from white (WM) and gray matter (GM) (69). Compared with the GM microglia, WM microglia expressed higher levels of HLA-DR, ApoE, CD68 and EMR1, which were consistent with the scRNA-seq results (69). Simultaneously comparing the single-cell phenotype of post-mortem cryopreserved huMG isolated from different brain regions (including the subventricular zone, thalamus, cerebellum, temporal lobe, and frontal lobe) using CyTOF has repeatedly confirmed microglial regional heterogeneity (11, 12). In these studies, we deeply characterised protein expression profiles of single huMG using multiple antibody panels determining around 60 proteins of interest. The results showed that human microglia constituted multiple distinct subtypes, with different abundance of each subset across the brain regions analysed. HuMG subset enriched in the subventricular zone and thalamus showed a phenotype with a high expression of CD68, CD11c, CD45, CD64, CD195, HLA-DR, and the proliferation markers cyclin A and cyclin B1. Interestingly, microglia clusters enriched in the temporal lobe and frontal lobe showed higher expression levels of CD206. Although we could not identify a cerebellum-specific microglia subset, the protein expression profile of single cerebellar microglia differed from that of the other regions (12). Of note, since subset identification by CyTOF depends very much on the antibody panel used, additional markers may be required to identify distinct signature of cerebellar huMG. It remains however to be investigated whether these identified sub-clusters of huMG enriched in respective

brain regions reflect a region-specific function or vulnerability of huMG to aging or CNS diseases, as it was proposed in mouse models (31). Nonetheless, unravelling the molecular machinery that shapes and/or maintains microglial regional diversity will allow for better understanding of the nature of homeostatic and diseased microglia in humans.

huMG diversity in diseased brains

In our recent study on human glioma brains, we combined two single-cell technologies, scRNA-seq and mass cytometry, to unravel signature changes of human glioma-associated microglia/macrophages (GAMs) (69). Results obtained from CyTOF consistently demonstrated phenotypic changes of P2Y₁₂/TMEM119-positive microglia in glioma brain biopsies, which were in line with the transcriptional changes identified by scRNA-seq. GAMs exhibited unique phenotypes distinguishing them from microglia which were isolated from control biopsies (the margins of epileptogenic focus). CyTOF revealed that microglia in glioma lesions became activated and expressed higher levels of HLA-DR, TREM2, ApoE, CD163, CD68, CD44, CD116, IL-6, GPR56 (also known as ADGRG1) and a number of other proteins such as GLUT5 and CD64. These results reproduced the transcriptomic signature of GAMs at the single cell protein level, and are in line with recently published findings (22). However, for some molecules with low transcript levels such as CX3CR1, CSF1R and FCGR1A, we found no change or even an increase in protein expression. These differences may be related to post-transcriptional regulatory mechanisms or differences in protein turnover. Our study underscores the synergy of using multiple single-cell omics techniques such as scRNA-seq and CyTOF to elucidate the interplay of both transcriptomics and proteomics in the context of microglia biology.

Similar to GAMs, we also detected the enrichment of microglia subsets that expressed higher levels of HLA-DR, CD44, CD68 and CD64 in active lesion (WM) of progressive multiple sclerosis (PMS), compared with normal appearing WM (NAWM) (13). Interestingly, we found in both brain pathologies an increased microglial expression of a cell-surface glycoprotein CD44, a molecule that has been proposed in mouse models as a marker to distinguish infiltrating myeloid cells (CD44⁺) from CNS-resident macrophages/microglia (CD44⁻) (40). It remains to be investigated whether the discrepancy between our findings in human brain and the previous study in mouse brain is disease- or species-related. Moreover, in this study (13), we applied meta-clustering analysis to CyTOF data obtained using three different antibody panels (a total of 74 markers). These panels included overlapping TYPE markers, which enabled comparison of cell subsets between experiments (see also “Antibody panel and staining” section). Using this strategy for in-depth immune phenotyping, we further identified microglial signatures in active lesions of progressive multiple sclerosis (PMS). Consistently, a cluster of homeostatic microglia was found

at lower frequency in the active lesion, whereas the lesion-enriched microglial clusters showed increased expression of proteins involved in phagocytic activity and microglial activation including CD45, CD14, CD11c, Clec7a (dectin-1) and its co-activator MS4A4A, CCR2, Fc gamma receptors (CD64 and CD32), CD91 (LRP1 or ApoE receptor), molecules involved in apoptosis-regulation CD95 (Fas), the receptor tyrosine kinase Axl, ATP-binding cassette (ABC) transporter A7 (ABCA7), inflammatory cytokines MIP-1 β (CCL4) and osteopontin (OPN, or *SPP1*), the myeloid inhibitory immunoreceptor SIRP α (CD172a) and its co-activator CD47 and immune regulatory function NFAT1 (a transcription factor regulating T-cell function) and galanin (13). Similarly, previous studies in experimental autoimmune encephalomyelitis (EAE) and human early MS revealed some of these lesion-associated signatures of microglia using single-cell transcriptomics (48). In our study (13), we additionally performed IMC on the same tissue blocks to validate the results obtained from single-cell suspension samples. Although using IMC we could reproduce some phenotypic changes of microglia determined by CyTOF in active lesions, in our opinion, a direct comparison between CyTOF and IMC remains technically challenging. This is mainly due to discrepancies between the areas of analysis, cell types analysed, tissue/cell quality and the number of compatible antibodies in one measurement. Even though results obtained from our studies are still limited and lack molecular mechanisms, it is tempting to speculate that, in diseased brains such as PMS and gliomas, microglia are most likely multi-functional. They show increased expression of molecules involved in maintenance of brain environment such as Axl (80), phospholipid transporter ABCA7 (1), HLA-DR, CD45, CD68 and/or the neuroprotective peptide galanin (82). Conversely, some microglia show increased expression of inflammatory mediators such as MIP-1 β and/or OPN (or *SPP1*).

In contrast, we could not detect any activation phenotype in microglia of donors with major depressive disorder (MDD) (11). Instead, CyTOF determination of 59 protein markers revealed enhanced expression of homeostatic markers such as TMEM119 and P2Y₁₂ of microglia in MDD brains. Moreover, we also detected increased microglial expression of CCR5, the receptor of chemokine CCL5, whose transcript level was found increased in cerebral cortex of MDD donors (24). None of the proinflammatory mediators analysed were different between MDD and control microglia. Also, the expression of HLA-DR and CD68 were found to be downregulated in the major cluster of microglia from MDD brains compared with controls.

Conclusions and future directions

Application of single-cell technologies to huMG study has offered new insights into microglial biology during development, homeostasis, aging and disease progression. As summarised in this

review, the power of multi-dimensional single-cell mass cytometry has been demonstrated in characterising huMG diversity in health and diseases. Our results underscore the heterogeneity and complexity of microglial phenotypes in human brains, and suggest potential similarities and differences of huMG responses in different CNS disorders. Therefore, the heterogeneity of huMG phenotypes might need to be considered when designing novel treatment interventions for CNS diseases (63). However, as mentioned, studies performed on human specimens have several common limitations. The sample size is usually very small due to the logistical difficulties and time-consuming nature of obtaining specimens from large cohorts of adequate control donors or patients with comparable pathologies. Post-mortem brain tissue of sufficient quality for CyTOF analysis is also difficult to obtain. The results obtained from such studies usually represent only one time point and one area of interest (this is especially true for biopsy samples). For some particular diseases or conditions such as psychiatric disorders or aging, it is difficult to obtain brain tissues from non-medicated donors, thus it is very challenging to control for some cofounders such as the effects of medication on huMG phenotypes. Comparing the effects of medication on similar cell types from different compartments (e.g. blood monocytes, CAMs and microglia) of the same donor may help to identify medication-related changes in huMG. Together, in order to achieve reliable datasets and to enable a proper interpretation of the results, considerations about collected cell types, quality of brain tissue and isolated single-cells, documentation of all possible cofounders and neuropathological diagnosis should be considered when designing the huMG experiments.

Although IMC is still not widely used for studying huMG biology, the first few studies on huMG (13, 60, 66) demonstrate the power of this technology to simultaneously characterize huMG subpopulations in their original tissue environment and to analyse the complex cellular network and cell-cell dynamics between different huMG subsets or between huMG and other CNS cell populations. This technology is a great complement to CyTOF analysis of isolated single cells, by which the information about cellular network and cell-cell interactions remain uninvestigated. In addition, in contrast to scRNA-seq, differentially regulated proteins may not completely be captured by mass cytometry analysis due to a limited number of target molecules. Conversely, transcriptomic measurements of single cells using scRNA-seq cannot completely discover the cell signalling pathways or the epigenetic heterogeneity that may drive huMG biology under disease conditions. Thus, using either single-cell technology may describe only some of the molecular phenotypes of microglia. To unravel a complete view of huMG phenotypic and functional diversity, future studies may require a concept of single-cell multimodal omics (scMulti-omics). ScMulti-omics technologies enable the measurement of multiple modalities, including DNA methylation, chromatin accessibility, RNA and protein expression, gene perturbation, and

spatial information, from a single cell (42, 46). Nevertheless, although such a concept may facilitate an identification of previously unknown subsets of huMG during both homeostasis and perturbation, characterisation of the distinct roles of these respective subsets remain experimentally challenging. Establishment of a stable *in vitro* huMG system is needed for functional analysis of huMG.

REFERENCES

1. Aikawa T, Ren Y, Yamazaki Y, Tachibana M, Johnson MR, Anderson CT et al (2019) ABCA7 haplodeficiency disturbs microglial immune responses in mouse brain. *Proc Natl Acad Sci U S A* **116**:23790–23796.
2. Ajami B, Samusik N, Wieghofer P, Ho PP, Crotti A, Bjornson Z et al (2018) Single-cell mass cytometry reveals distinct populations of brain myeloid cells in mouse neuroinflammation and neurodegeneration models. *Nat Neurosci* **21**:541–551.
3. Ali HR, Jackson HW, Zanotelli VRT, Danenberg E, Fischer JR, Bardwell H et al (2020) Imaging mass cytometry and multiplatform genomics define the phenogenomic landscape of breast cancer. *Nat Cancer* **1**:163–175.
4. Amir el-AD, Davis KL, Tadmor MD, Simonds EF, Levine JH, Bendall SC et al (2013) t-SNE enables visualization of high dimensional single-cell data and reveals phenotypic heterogeneity of leukemia. *Nat Biotechnol* **31**:545–552.
5. Bagwell CB, Hunsberger B, Hill B, Herbert D, Bray C, Selvanantham T et al (2020) Multi-site reproducibility of a human immunophenotyping assay in whole blood and peripheral blood mononuclear cells preparations using CyTOF technology coupled with Maxpar Pathsetter, an automated data analysis system. *Cytometry B Clin Cytom* **98**:146–160.
6. Becht E, McInnes L, Healy J, Dutertre CA, Kwok IWH, Ng LG et al (2019) Dimensionality reduction for visualizing single-cell data using UMAP. *Nat Biotechnol* **37**:38–44.
7. Bendall SC, Simonds EF, Qiu P, Amir el-AD, Krutzik PO, Finck R et al (2011) Single-cell mass cytometry of differential immune and drug responses across a human hematopoietic continuum. *Science* **332**:687–96.
8. Berg S, Kutra D, Kroeger T, Straehle CN, Kausler BX, Haubold C et al (2019) Ilastik: interactive machine learning for (bio)image analysis. *Nat Methods* **16**:1226–1232.
9. Beutner C, Linnartz-Gerlach B, Schmidt SV, Beyer M, Mallmann MR, Staratschek-Jox A et al (2013) Unique transcriptome signature of mouse microglia. *Glia* **61**:1429–1442

- Accepted Article
10. Böttcher C, Fernández-Zapata C, Schlickeiser S, Kunkel D, Schulz AR, Mei HE *et al* (2019) Multi-parameter immune profiling of peripheral blood mononuclear cells by multiplexed single-cell mass cytometry in patients with early multiple sclerosis. *Sci Rep* **9**:19471.
 11. Böttcher C, Fernández-Zapata C, Snijders GJL, Schlickeiser S, Sneeboer MAM, Kunkel D *et al* (2020) Single-cell mass cytometry of microglia in major depressive disorder reveals a non-inflammatory phenotype with increased homeostatic marker expression. *Transl Psychiatry* **10**, 310.
 12. Böttcher C, Schlickeiser S, Sneeboer MAM, Kunkel D, Knop A, Paza E *et al* (2019) Human microglia regional heterogeneity and phenotypes determined by multiplexed single-cell mass cytometry. *Nat Neurosci* **22**:78–90.
 13. Böttcher C, van der Poel M, Fernández-Zapata C, Schlickeiser S, Leman JKH, Hsiao CC *et al* (2020) Single-cell mass cytometry reveals complex myeloid cell composition in active lesions of progressive multiple sclerosis. *Acta Neuropathol Commun* **8**:136.
 14. Carpenter AE, Jones TR, Lamprecht MR, Clarke C, Kang IH, Friman O *et al* (2006) CellProfiler: image analysis software for identifying and quantifying cell phenotypes. *Genome Biol* **7**:R100.
 15. Carvajal-Hausdorf DE, Patsenker J, Stanton KP, Villarroel-Espindola F, Esch A, Montgomery RR *et al* (2019) Multiplexed (18-Plex) measurement of signaling targets and cytotoxic T cells in Trastuzumab-treated patients using imaging mass cytometry. *Clin Cancer Res* **25**:3054–3062.
 16. Chatterjee D, Sarkar PK (1984) Isolation of protoplasmic astrocytes: a procedure based on controlled trypsin digestion. *J Neurochem* **42**:1229–1234.
 17. Cheung P, Vallania F, Warsinske HC, Donato M, Schaffert S, Chang SE *et al* (2018) Single-cell chromatin modification profiling reveals increased epigenetic variations with aging. *Cell* **173**:1385–1397.e14.
 18. Chevrier S, Crowell HL, Zanotelli VRT, Engler S, Robinson MD, Bodenmiller B (2018) Compensation of Signal Spillover in Suspension and Imaging Mass Cytometry. *Cell Syst* **6**:612–620.e5.
 19. Damond N, Engler S, Zanotelli VRT, Schapiro D, Wasserfall CH, Kusmartseva I *et al* (2019) A Map of human type 1 diabetes progression by imaging mass cytometry. *Cell Metab* **29**:755–768.e5.
 20. Fienberg HG, Simonds EF, Fantl W J, Nolan GP, Bodenmiller B (2012) A platinum-based covalent viability reagent for single-cell mass cytometry. *Cytometry A* **81A**:467–475.
 21. Finck R, Simonds EF, Jager A, Krishnaswamy S, Sachs K, Fantl W *et al* (2013) Normalization of mass cytometry data with bead standards. *Cytometry A* **83**:483–494.

- Accepted Article
22. Friebel E, Kapolou K, Unger S, Núñez NG, Utz S, Rushing EJ *et al* (2020) Single-cell mapping of human brain cancer reveals tumor-specific instruction of tissue-invading leukocytes. *Cell* **181**:1626–1642.
 23. Galatro TF, Holtman IR, Lerario AM, Vainchtein ID, Brouwer N, Sola PR *et al* (2017) Transcriptomic analysis of purified human cortical microglia reveals age-associated changes. *Nat Neurosci* **20**:1162–1171.
 24. Gandal MJ, Zhang P, Hadjimichael E, Walker RL, Chen C, Liu S, *et al* (2018) Transcriptome-wide isoform-level dysregulation in ASD, schizophrenia, and bipolar disorder. *Science* **362**(6420):eaat8127.
 25. Gerdtsso E, Pore M, Thiele JA, Gerdtsso AS, Malihi PD, Nevarez R *et al* (2018) Multiplex protein detection on circulating tumor cells from liquid biopsies using imaging mass cytometry. *Converg Sci Phys Oncol* **4**:015002.
 26. Gertig U, Hanisch UK (2014) Microglia diversity by responses and responders. *Front Cell Neurosci* **8**:101.
 27. Giesen C, Wang HA, Schapiro D, Zivanovic N, Jacobs A, Hattendorf B *et al* (2014) Highly multiplexed imaging of tumor tissues with subcellular resolution by mass cytometry. *Nat Methods* **11**:417–422.
 28. Ginhoux F, Greter M, Leboeuf M, Nandi S, See P, Gokhan S *et al* (2010) Fate mapping analysis reveals that adult microglia derive from primitive macrophages. *Science* **330**:841–845.
 29. Goldmann T, Wieghofer P, Jordão MJC, Prutek F, Hagemeyer N, Frenzel K *et al* (2016) Origin, fate and dynamics of macrophages at central nervous system interfaces. *Nat Immunol* **17**:797–805.
 30. Gosselin D, Skola D, Coufal NG, Holtman IR, Schlachetzki JCM, Sajti E *et al* (2017) An environment-dependent transcriptional network specifies human microglia identity. *Science* **356**:eaal3222.
 31. Grabert K, Michoel T, Karavolos MH, Clohisey S, Baillie JK, Stevens MP *et al* (2016) Microglial brain region-dependent diversity and selective regional sensitivities to aging. *Nat Neurosci* **19**:504–516.
 32. Han G, Chen SY, Gonzalez VD, Zunder ER, Fantl WJ, Nolan GP (2017) Atomic mass tag of bismuth-209 for increasing the immunoassay multiplexing capacity of mass cytometry. *Cytometry A* **91**:1150–1163
 33. Han G, Spitzer MH, Bendall SC, Fantl WJ, Nolan GP (2018) Metal-isotope-tagged monoclonal antibodies for high-dimensional mass cytometry. *Nat Protoc* **13**:2121–2148.

- Accepted Article
34. Hartmann FJ, Babdor J, Gherardini PF, Amir ED, Jones K, Sahaf B *et al* (2019) Comprehensive immune monitoring of clinical trials to advance human immunotherapy. *Cell Rep* **28**:819–831.e4.
 35. Hartmann FJ, Simonds EF, Bendall SC (2018) A universal live cell barcoding-platform for multiplexed human single cell analysis. *Sci Rep* **8**:10770.
 36. Hartmann FJ, Simonds EF, Vivanco N, Bruce T, Borges L, Nolan GP *et al* (2019) Scalable conjugation and characterization of immunoglobulins with stable mass isotope reporters for single-cell mass cytometry analysis. *Methods Mol Biol* **1989**:55–81.
 37. Jordão MJC, Sankowski R, Brendecke SM, Sagar, Locatelli G, Tai Y-H *et al* (2019) Single-cell profiling identifies myeloid cell subsets with distinct fates during neuroinflammation. *Science* **363**:eaat7554.
 38. Kierdorf K, Erny D, Goldmann T, Sander V, Schulz C, Perdigero EG *et al* (2013) Microglia emerge from erythromyeloid precursors via Pu.1- and Irf8-dependent pathways. *Nat Neurosci* **16**:273–280.
 39. Kleinstuber K, Corleis B, Rashidi N, Nchinda N, Lisanti A, Cho JL *et al* (2016) Standardization and quality control for high-dimensional mass cytometry studies of human samples. *Cytometry A* **89**: 903–913.
 40. Korin B, Ben-Shaanan TL, Schiller M, Dubovik T, Azulay-Debby H, Boshnak NT *et al* (2017) High-dimensional, single-cell characterization of the brain's immune compartment. *Nat Neurosci* **20**:1300–1309.
 41. Kracht L, Borggrewe M, Eskandar S, Brouwer N, Chuva de Sousa Lopes SM, Laman JD *et al* (2020) Human fetal microglia acquire homeostatic immune-sensing properties early in development. *Science* **369**:530–537.
 42. Lake BB, Chen S, Sos BC, Fan J, Kaeser GE, Yung YC *et al* (2018) Integrative single-cell analysis of transcriptional and epigenetic states in the human adult brain. *Nat Biotechnol* **36**:70–80.
 43. Leipold MD, Newell EW, Maecker HT (2015) Multiparameter phenotyping of human PBMCs using mass cytometry. *Methods Mol Biol* **1343**:81–95.
 44. Leipold MD, Obermoser G, Fenwick C, Kleinstuber K, Rashidi N, McNevin JP *et al* Comparison of CyTOF assays across sites: results of a six-center pilot study. *J Immunol Methods* **453**:37–43.
 45. Li N, van Unen V, Abdelaal T, Guo N, Kasatskaya SA, Ladell K *et al* (2019) Memory CD4⁺ T cells are generated in the human fetal intestine. *Nat Immunol* **20**:301–312.
 46. Ma A, McDermaid A, Xu J, Chang Y, Ma Q (2020) Integrative methods and practical challenges for single-cell multi-omics. *Trends Biotechnol* **38**:1007–1022.

47. Maaten L Van Der, Hinton G (2008) Visualizing data using t-SNE. *J Mach Learn Res* **9**:2579–2605.
48. Masuda T, Sankowski R, Staszewski O, Böttcher C, Amann L, Scheiwe C et al (2019) Spatial and temporal heterogeneity of mouse and human microglia at single-cell resolution. *Nature* **566**:388–392.
49. Masuda T, Sankowski R, Staszewski O, Prinz M (2020) Microglia heterogeneity in the single-cell era. *Cell Rep* **30**:1271–1281.
50. Mei HE, Leipold MD, Maecker HT (2016) Platinum-conjugated antibodies for application in mass cytometry. *Cytometry A* **89**:292–300.
51. Melief J, Sneeboer MA, Litjens M, Ormel PR, Palmen SJ, Huitinga I et al (2016) Characterizing primary human microglia: a comparative study with myeloid subsets and culture models. *Glia* **64**:1857–1868.
52. Mildner A, Huang H, Radke J, Stenzel W, Priller J (2017) P2Y12 receptor is expressed on human microglia under physiological conditions throughout development and is sensitive to neuroinflammatory diseases. *Glia* **65**:375–387.
53. Mingueneau M, Krishnaswamy S, Spitzer MH, Bendall SC, Stone EL, Hedrick SM et al (2014) Single-cell mass cytometry of TCR signaling: amplification of small initial differences results in low ERK activation in NOD mice. *Proc Natl Acad Sci U S A* **111**:16466–16471.
54. Mizee MR, Miedema SS, van der Poel M, Adelia, Schuurman KG, van Strien ME et al (2017) Isolation of primary microglia from the human post-mortem brain: effects of ante- and post-mortem variables. *Acta Neuropathol Commun* **5**:16.
55. Mizutani M, Pino PA, Saederup N, Charo IF, Ransohoff RM, Cardona AE (2012) The fractalkine receptor but not CCR2 is present on microglia from embryonic development throughout adulthood. *J Immunol* **188**:29–36.
56. Moore CS, Ase AR, Kinsara A, Rao VT, Michell-Robinson M, Leong SY et al (2015) P2Y12 expression and function in alternatively activated human microglia. *Neuro Immunol Neuroinflamm* **2**:e80.
57. Nowicka M, Krieg C, Crowell HL, Weber LM, Hartmann FJ, Guglietta S et al (2017) CyTOF workflow: differential discovery in high-throughput high-dimensional cytometry datasets. Version 3. *F1000Res* **6**:748.
58. Olah M, Raj D, Brouwer N, De Haas AH, Eggen BJL, Den Dunnen WFA et al (2012) An optimized protocol for the acute isolation of human microglia from autopsy brain samples. *Glia* **60**:96–111.
59. Ornatsky OI, Lou X, Nitz M, Schäfer S, Sheldrick WS, Baranov VI et al (2008) Study of cell antigens and intracellular DNA by identification of element-containing labels and

- metallointercalators using inductively coupled plasma mass spectrometry. *Anal Chem* **80**:2539–47.
60. Park C, Ponath G, Levine-Ritterman M, Bull E, Swanson EC, De Jager PL *et al* (2019) The landscape of myeloid and astrocyte phenotypes in acute multiple sclerosis lesions. *Acta Neuropathol Commun* **7**:130.
 61. Parkhurst CN, Yang G, Ninan I, Savas JN, Yates JR, Lafaille JJ *et al* (2013) Microglia promote learning-dependent synapse formation through brain-derived neurotrophic factor. *Cell* **155**:1596–1609.
 62. Peferoen LA, Vogel DY, Ummenthum K, Breur M, Heijnen PD, Gerritsen WH *et al* (2015) Activation status of human microglia is dependent on lesion formation stage and remyelination in multiple sclerosis. *J Neuropathol Exp Neurol* **74**:48–63.
 63. Priller J, Prinz M (2019) Targeting microglia in brain disorders. *Science* **365**(6448):32–33.
 64. Prinz M, Jung S, Priller J (2019) Microglia biology: one century of evolving concepts. *Cell* **179**:292–311.
 65. R Core Team (2017) R: A language and environment for statistical computing. *R Foundation for Statistical Computing*, Vienna, Austria. <https://www.R-project.org/>.
 66. Ramaglia V, Sheikh-Mohamed S, Legg K, Park C, Rojas OL, Zandee S *et al* (2019) Multiplexed imaging of immune cells in staged multiple sclerosis lesions by mass cytometry. *Elife* **8**:e48051.
 67. Rodriguez-Zas SL, Wu C, Southey BR, O'Connor JC, Nixon SE, Garcia R *et al* (2018) Disruption of microglia histone acetylation and protein pathways in mice exhibiting inflammation-associated depression-like symptoms. *Psychoneuroendocrinology* **97**:47–58.
 68. Samusik N, Good Z, Spitzer MH, Davis KL, Nolan GP (2016) Automated mapping of phenotype space with single-cell data. *Nat Methods* **13**:493–496.
 69. Sankowski R, Böttcher C, Masuda T, Geirsdottir L, Sagar, Sindram E, Seredenina T *et al* (2019) Mapping microglia states in the human brain through the integration of high-dimensional techniques. *Nat Neurosci* **22**:2098–2110.
 70. Schapiro D, Jackson HW, Raghuraman S, Fischer JR, Zanotelli VRT, Schulz D *et al* (2017) histoCAT: analysis of cell phenotypes and interactions in multiplex image cytometry data. *Nat Methods* **14**:873–876.
 71. Schulz AR, Baumgart S, Schulze J, Urbicht M, Grützkau A, Mei HE (2019) Stabilizing antibody cocktails for mass cytometry. *Cytometry A* **95**:910–916.
 72. Schulz C, Perdigero EG, Chorro L, Szabo-Rogers H, Cagnard N, Kierdorf K *et al* (2012) A lineage of myeloid cells independent of Myb and hematopoietic stem cells. *Science* **336**, 86–90.

73. Schuyler RP, Jackson C, Garcia-Perez JE, Baxter RM, Ogolla S, Rochford R *et al* (2019) Minimizing batch effects in mass cytometry data. *Front Immunol* **10**:2367.
74. Sierra A, Encinas JM, Deudero JJP, Chancey JH, Enikolopov G, Overstreet-Wadiche LS *et al* (2010) Microglia shape adult hippocampal neurogenesis through apoptosis-coupled phagocytosis. *Cell Stem Cell* **7**:483–495.
75. Takahashi C, Au-Yeung A, Fuh F, Ramirez-Montagut T, Bolen C, Mathews W *et al* (2017) Mass cytometry panel optimization through the designed distribution of signal interference. *Cytometry A* **91**:39–47.
76. Van Gassen S, Callebaut B, Van Helden MJ, Lambrecht BN, Demeester P, Dhaene T (2015) FlowSOM: Using self-organizing maps for visualization and interpretation of cytometry data. *Cytometry A* **87**:636–645.
77. Van Gassen S, Gaudilliere B, Angst MS, Saeys Y, Aghaeepour N (2020) CytoNorm: A normalization algorithm for cytometry data. *Cytometry A* **97**:268–278.
78. Wählby C, Erlandsson F, Bengtsson E, Zetterberg A (2002) Sequential immunofluorescence staining and image analysis for detection of large numbers of antigens in individual cell nuclei. *Cytometry* **47**:32–41.
79. Wang YJ, Traum D, Schug J, Gao L, Liu C; HPAP Consortium *et al* (2019) Multiplexed in situ imaging mass cytometry analysis of the human endocrine pancreas and immune system in type 1 diabetes. *Cell Metab* **29**:769–783.e4.
80. Weinger JG, Brosnan CF, Loudig O, Goldberg MF, Macian F, Arnett HA *et al* (2011) Loss of the receptor tyrosine kinase Axl leads to enhanced inflammation in the CNS and delayed removal of myelin debris during experimental autoimmune encephalomyelitis. *J Neuroinflammation* **8**:49.
81. Wilkerson MD, Hayes DN (2010) *ConsensusClusterPlus*: a class discovery tool with confidence assessments and item tracking. *Bioinformatics* **26**:1572–1573.
82. Wraith DC, Pope R, Butzkueven H, Holder H, Vanderplank P, Lowrey P *et al* (2009) A role for galanin in human and experimental inflammatory demyelination. *Proc Natl Acad Sci U S A* **106**:15466–15471.
83. Xu D, Robinson AP, Ishii T, Duncan DS, Alden TD, Goings GE *et al* (2018) Peripherally derived T regulatory and $\gamma\delta$ T cells have opposing roles in the pathogenesis of intractable pediatric epilepsy. *J Exp Med* **215**:1169–1186.
84. Zhao Y, Uduman M, Siu JHY, Tull TJ, Sanderson JD, Wu YB *et al* (2018) Spatiotemporal segregation of human marginal zone and memory B cell populations in lymphoid tissue. *Nat Commun* **9**:3857.

85. Ziegler JF, Böttcher C, Letizia M, Yerinde C, Wu H, Freise I *et al* (2019) Leptin induces TNF α -dependent inflammation in acquired generalized lipodystrophy and combined Crohn's disease. *Nat Commun* **10**:5629.
86. Zunder ER, Finck R, Behbehani GK, Amir el-AD, Krishnaswamy S, Gonzalez VD *et al* (2015) Palladium-based mass tag cell barcoding with a doublet-filtering scheme and single-cell deconvolution algorithm. *Nat Protoc* **10**:316–333.

FIGURE LEGENDS

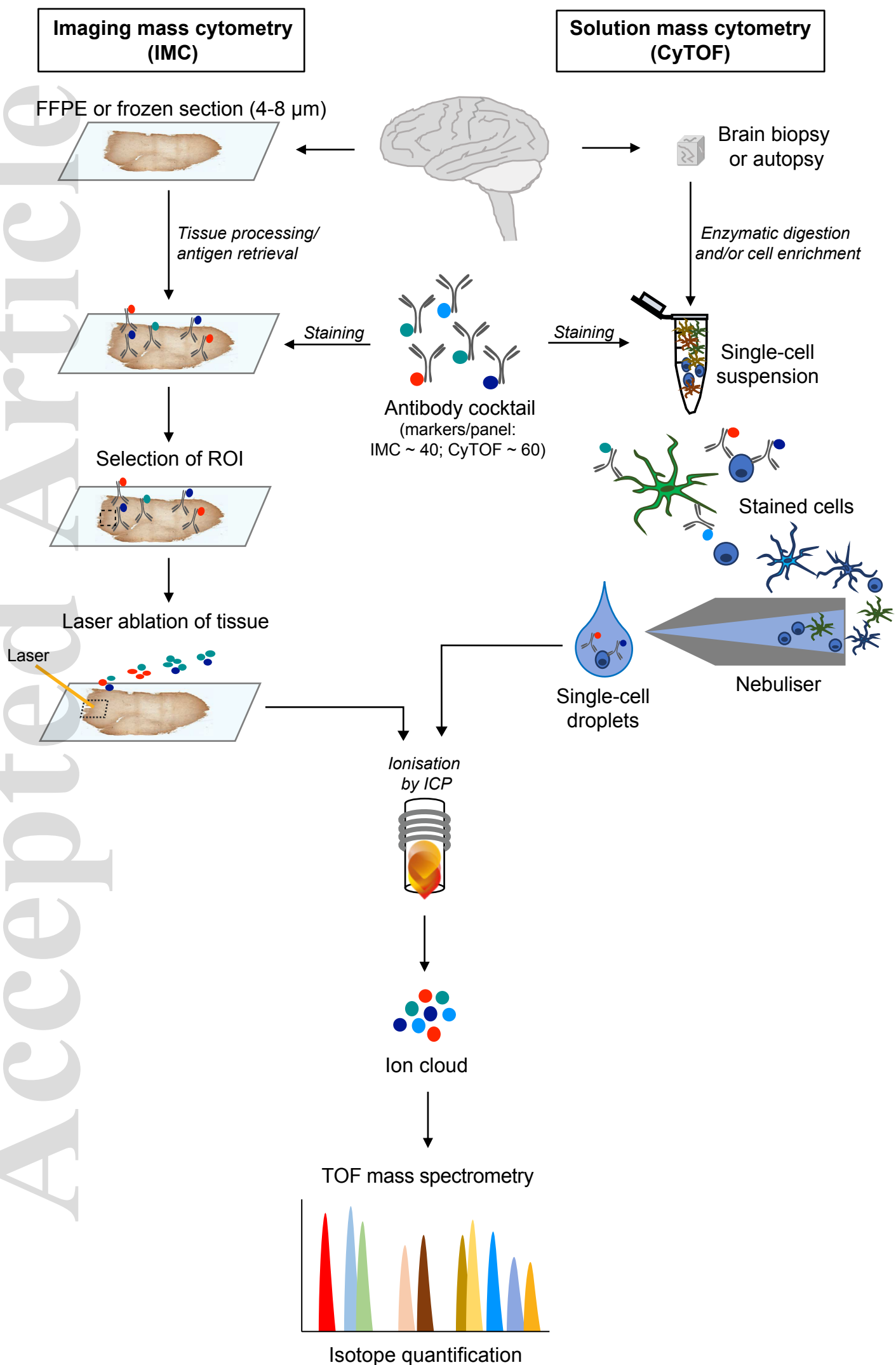
Figure 1 Analytical workflow for mass cytometry (CyTOF) and imaging mass cytometry (IMC). In IMC analysis, tissue of interest is sliced and slide mounted. Depending on the state of the tissue, antigen retrieval or de-paraffinisation steps may be required. The slide is stained with a panel of antibodies conjugated to heavy metal isotopes. Regions of interest (ROI) are selected, and ablated μm by μm by a UV laser. The tissue and associated isotopes are introduced into the mass cytometer and ionised by inductively coupled plasma (ICP). For CyTOF measurement, biopsy or autopsy samples are taken, and processed into a single cell suspension. Depending on the tissue and cells of interest, this may involve enzymatic digestion or cell enrichment. The single cell suspension is stained with a cocktail of antibodies conjugated to heavy metal isotopes (usually up to 40), and then the stained cells are passed through a nebuliser to create single cell droplets. Subsequently, the droplets are ionised by ICP. The ion cloud from each μm (IMC) or droplet (CyTOF) is analysed using time-of-flight (TOF) mass spectrometry, to quantify which ions are associated with a single spot or droplet.

Figure 2 Characterisation of huMG using mass cytometry. Donor (for brain autopsies) and/or patient (for biopsy tissues) cohorts including the control group are selected depending on accessibility, ethics and the experimental questions to be investigated. HuMG and other immune cells (optional) of interest can be isolated from different brain regions/compartments. At least 10^4 cells per aliquot is recommended. A cell isolation strategy is chosen based on tissue types and cell type abundance and/or vulnerability (for example to enzymatic digestion). To minimise the contamination of isolated huMG fraction by remaining myelin and cell debris, an additional step of cell enrichment such as the fluorescence- or magnetic-activated cell sorting can be included. Isolated cells can be either analysed directly or cryopreserved as either live or fixed cells. In the case of immediate analysis, a workflow/protocol for sample normalisation is required. Live/dead fixable staining can be performed prior to cell fixation (optional) and cryopreservation. To reduce inter-run and technical variation, samples can be barcoded, pooled, stained and acquired as a

single sample. It is advisable to include anchor samples to facilitate the data normalisation, and negative and positive control cells to enable the validation of antibody affinity and specificity.

Figure 3 Data analysis workflow for IMC and CyTOF. Schematic representation of IMC and CyTOF data analysis. After acquisition, raw data must undergo some pre-processing steps, these include single-cell segmentation (IMC), sample de-barcoding (CyTOF) and signal spillover compensation and arcsinh transformation (IMC and CyTOF). Then visualisation of the data can be done using different algorithms such as tSNE, UMAP and FDL, or using high-dimensional image visualisation in IMC. Finally, unsupervised clustering can be performed and the results plotted back into reduced dimensionality plots and phenotypic heatmaps.

Figure 4 HuMG heterogeneity in health and disease determined by mass cytometry. Markers used to distinguish circulating immune cells from microglia, CAMs and myeloid cell-derived macrophages (MDMs), as well as markers whose expression were changed in glioma or PMS brains are summarised (see refs. 10, 11, 12, 13, 22, 69).





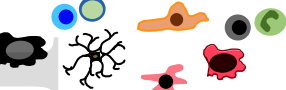
Donor/Patient cohort

- Accessibility and ethics
- Experimental questions
- Disease-specific context
- Control group



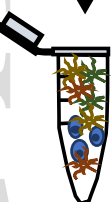
Sample collection

- Brain regions
- Multiple cell types
- Multiple compartments



Sample processing

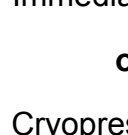
- Percoll density gradient centrifugation
- With or without enzymatic digestion
- With or without cell enrichment



Immediate analysis

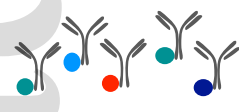
- Inter-run variation
- Normalization

or



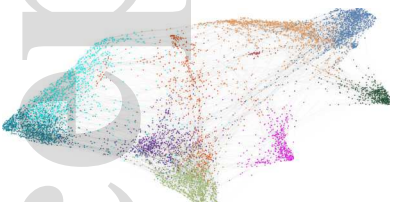
Cryopreservation

- As either live or fixed cells
- Live/dead fixable staining



Barcode,
pooling of multiple samples
and staining

- Live/surface barcoding
- Fixed/intracellular barcoding
- The use of anchor samples
- Negative and positive control



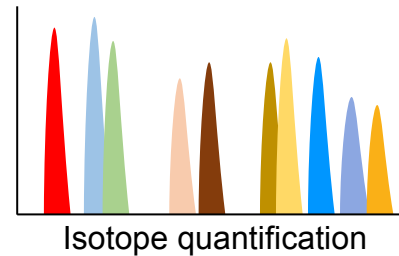
Acquisition and data analysis

- Computation capacity
- Normalization

Step

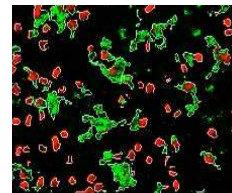
Processing and analysis

Acquisition

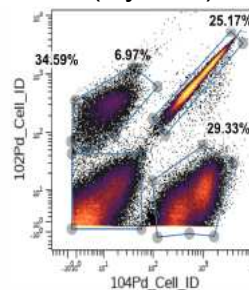


Pre-processing

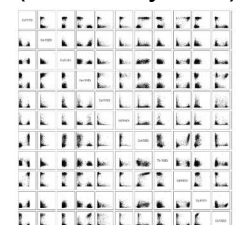
Single-cell segmentation
(IMC)



De-barcoding
(CyTOF)

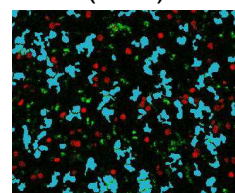


Signal compensation
(IMC & CyTOF)

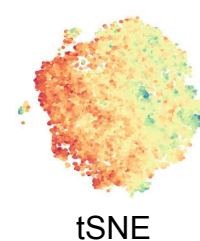


Unsupervised clustering
and
visualisation

Image visualisation
(IMC)



Dimensionality reduction plots
(IMC & CyTOF)



tSNE

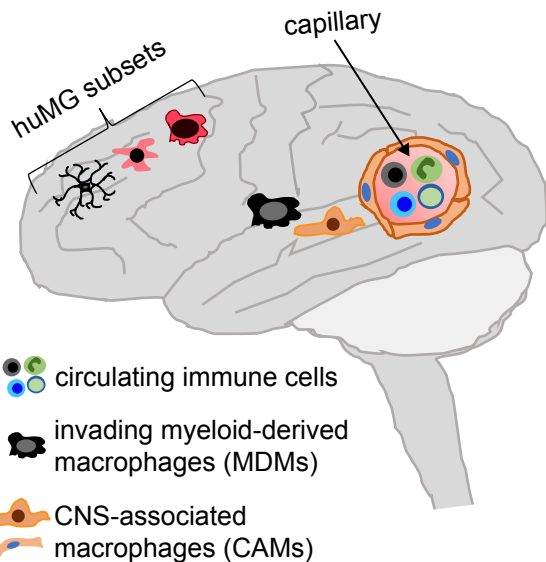


UMAP



FDL

Accepted Article



Lineage markers discriminating T cells, B-/plasma cells, DCs, neutrophils, NK cells and monocytes

CADM1, CCR2, CD1c, CD3, CD11b, CD11c, CD14, CD16, CD19, CD33, CD38, CD49d, CD45RA, CD56, CD64, CD66b, CD123, CD141, CX3CR1, HLA-DR, Fc ϵ R1,

	Microglia	CAMs	MDMs
negative	CCR2, CCR7, CD123, CD141, CD163, CD169, CD19, CD1c, CD206, CD3, CD35, CD36, CD37, CD38, CD44, CD45RA, CD49d, CD66b, Clec12A, FC ϵ R1, GM-CSF, IRF4, MIP β , MRP14 (S100A9)	CCR7, CD123, CD141, CD169, CD19, CD1c, CD3, CD4, CD34, CD35, Clec7a, CD36, CD37, CD44, CD66b, CD8, Clec12A, GLUT5, GM-CSF, GPR56, MIP β , P2Y ₁₂ , TMEM119, TNF, TREM2	CCR7, CD116, CD123, CD19, CD1c, CD3, CD4, CD34, Clec7a, CD37, CD44, CD66b, CD8, galanin, GLUT5, GPR56, IRF4, MIP β , P2Y ₁₂ , TMEM119, TNF, TREM2
low positive or subset-dependent	ABCA7, ApoE, AXL, CADM1, CD116, CD14, CD16, CD33, CD34, Clec7a (CD369), CD4, CD40, CD45, CD47, CD56, CD61, CD8, CD86, CD95, galanin, CD54, MS4A4A, NFAT1, OPN (SPP1), TNF	ABCA7, ApoE, AXL, CADM1, CCR2, CD116, CD16, CD33, CD38, CD40, CD44, CD47, CD56, CD61, CD8, CD74, CD86, CD95, EMR1, galanin, CD54, IRF4, IRF8, MS4A4A, NFAT1, OPN (SPP1)	ABCA7, ApoE, AXL, CADM1, CD16, CD38, CD40, CD44, CD33, CD56, CD61, CD8, CD74, CD86, EMR1, CD54, GM-CSF, IRF8, MS4A4A, NFAT1, OPN (SPP1)
positive	C/EBP α , CCR5, CD11b, CD11c, CD115, CD172a, CD18, CD32, CD64, CD68, CD74, CD88, CD91, CX3CR1, CXCR3, EMR1, GLUT5, GPR56, HLA-DR, IRF8, MERTK, P2Y ₁₂ , TGF β , TMEM119, TREM2	C/EBP α , CCR5, CD11b, CD11c, CD115, CD14, CD163, CD169, CD172a, CD18, CD206, CD32, CD35, CD36, CD45, CD64, CD68, CD91, CX3CR1, CXCR3, HLA-DR, MERTK, TGF β	C/EBP α , CCR5, CD11b, CD11c, CD115, CD14, CD141, CD163, CD169, CD172a, CD18, CD206, CD32, CD35, CD36, CD45, CD45RA, CD49d, CD47, CD64, CD68, CD88, CD91, CD95, Clec12A, CX3CR1, CXCR3, HLA-DR, MERTK, TGF β , MRP14 (S100A9)
regulated under CNS pathology	ABCA7, ApoE, AXL, CCR5, CD11c, CD14, CD16, CD163, CD169, CD172a, CD19, CD206, CD3, CD33, Clec7A, CD36, CD44, CD45, CD47, CD61, CD64, CD68, CD74, CD91, CD95, CX3CR1, EMR1, galanin, GLUT5, GM-CSF, GPR56, HLA-DR, IRF8, MIP β , MS4A4A, NFAT1, P2Y ₁₂ , OPN, TMEM119, TNF, TREM2	NA	NA
References	10 , 11 , 12 , 13 , 22 , 69		